

EFFECTIVE STRESS METHOD FOR DYNAMIC RESPONSE ANALYSIS
OF HORIZONTALLY LAYERED SOILS

S. K. Sarma (I)
C. P. Tsatsanifos (II)

Presenting Author : S. K. Sarma

SUMMARY

A method of analysis in terms of effective stresses is developed, aiming in the determination of the dynamic response of saturated, horizontally layered sandy soils when subjected to earthquake loading. A direct nonlinear analysis based on a hyperbolic stress-strain law and employing dynamic pore pressure parameters is performed. The method is applied to study the response differences owing to the use of a total stress or an effective stress analysis, as well as to study the effects of soil properties, bed-rock motion intensity and existence of surface surcharge, on the response characteristics of a soil deposit.

INTRODUCTION

The dynamic response of horizontally layered soils has been the subject of considerable interest and research, and many analytical and numerical procedures have been developed for this purpose. These procedures differ in the simplifying assumptions that are made, in the idealization of the physical system, in the representation of the stress-strain behaviour of soils, in the manner in which the development of excess pore pressure during the earthquake is taken into account, and in the methods used to integrate the equation of motion.

The nonlinear behaviour and the development of excess pore pressure in soils under cyclic loading is very pronounced. As such, it is essential to apply a nonlinear effective stress analysis which takes into account the effects of this pore pressure increase as the earthquake progresses. Recently, several methods of effective stress response analysis have been proposed (Ref. 1,2,3,5,6,7,8). These methods should be compared mainly on their effectiveness in approximating the nonlinear stress-strain behaviour of the soil and the pore pressure build up. Herein, a new method is presented, based on the coupling of dynamic soil response and pore pressure response.

CONSTITUTIVE RELATION

The constitutive relation presented by Tsatsanifos (Ref. 11) and Sarma and Tsatsanifos (Ref.10) was used. During an earthquake a sand deposit is subjected to an irregular loading pattern, which consists of intervals of loading, unloading, reloading or reverse loading. The stress-strain behaviour of the sand in each loading pattern is different. It is assumed that during the initial loading, and up to the point of the first

-
- (I) Lecturer, Imperial College, University of London, U.K.
(II) Consulting Geotechnical Engineer, Athens, Greece.

load reversal, a hyperbolic stress-strain path is followed. This path can be described by the equation

$$\tau = \frac{G_{\max} \cdot \gamma}{1 + \frac{G_{\max} \cdot \gamma}{\tau_{\max}}} \quad (1)$$

in which G_{\max} is the initial maximum tangent shear modulus and τ_{\max} is the asymptote of the hyperbola. Expressions for the parameters G_{\max} and τ_{\max} have been proposed by Hardin and Drnevich (Ref. 4)

It is also assumed that during unloading, and up to the point of total load reversal, a linear stress-strain path is followed, with a modulus equal to the initial modulus of the virgin curve. When reloading occurs before total load reversal, the linear path is followed until the last hyperbolic path is crossed, Fig. 1. From that point on, this hyperbola is followed until the next load reversal.

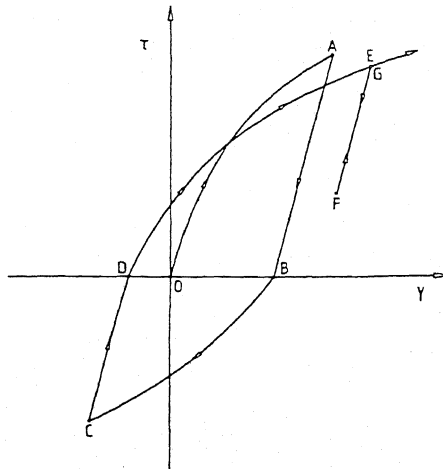


Fig. 1 Modified Hyperbolic Model

Finally, when the stress-strain path crosses the strain axis and complete load reversal occurs, the linear path is abandoned and a hyperbolic path is followed again. This new hyperbola is fitted from the crossing point to the asymptote defined by the virgin curve, with an initial maximum tangent shear modulus.

$$G_m = G_{\max} \left[1 + \frac{G_{\max} (\gamma - \gamma_r)}{(\text{sgn} \dot{\gamma}) \tau_{\max} - \tau_r} \right]^{-2} \quad (2)$$

in which γ is the shear strain of the crossing point, γ_r and τ_r are the coordinates of the last load reversal point, and $(sg\dot{x})$ denotes the sign of the response velocity at the particular time instance. Hence, the expression for any reloading and reverse loading curve is

$$\tau = \frac{G_m (\gamma - \gamma_r)}{1 + \frac{G_m (\gamma - \gamma_r)}{(sg\dot{x})\tau_{max}}} \quad (3)$$

where γ_r is the shear strain of the crossing point

PORE PRESSURE RISE MODEL

The modified dynamic pore pressure parameter model proposed by Tsatsanifos and Sarma (Ref.12) is used. The excess pore pressure increase Δu , up to the Nth cycle of loading, due to the application of shear stress τ is

$$\frac{\Delta u}{\sigma'_{vo}} = \left[\left(\frac{C_1}{1 - C_2 \frac{\tau}{\sigma'_{vo}}} \right)^{\frac{1}{2}} + (C_3 + C_4 \frac{\tau}{\sigma'_{vo}}) \log N \right]^2 \frac{\tau}{\sigma'_{vo}} \quad (4)$$

in which σ'_{vo} is the initial vertical effective stress and C_1, C_2, C_3 and C_4 soil parameters.

Using Eq. 4, it is possible to predict the pore pressure rise under a given cyclic loading up to any number of uniform cycles. In case of nonuniform loading a method based on the assumption that the pore pressure increase during each cycle depends on the pore pressure level existing at the beginning of that cycle is used (Ref. 9).

COUPLED EFFECTIVE STRESS MODEL

Coupling of the stress-strain model with the pore pressure rise model results in an effective stress-strain relationship the parameters of which are updated at each time step in order to be compatible with the current level of effective stress. If G_{mn} is the maximum shear modulus and τ_{mn} is the maximum allowable shear stress at the end of the Nth cycle of loading, then

$$G_{mn} = G_{max} \left(\frac{\sigma'_v}{\sigma'_{vo}} \right)^{\frac{1}{2}} \quad (5)$$

$$\tau_{mn} = \tau_{max} \cdot \frac{\sigma'_v}{\sigma'_{v0}} \quad (6)$$

Hence, the updated form of the hyperbolic stress-strain path (Eq. 3) is given by

$$\tau = \frac{G_{mn} (\gamma - \gamma_r)}{1 + \frac{G_{mn} (\gamma - \gamma_r)}{(sg\dot{x})\tau_{mn}}} \quad (7)$$

It has been noted (2) that most of the volume changes during drained cyclic loading tests and the pore pressure rise during undrained tests occur during the unloading parts of any load cycle. Accordingly, modifications to the parameters of the stress-strain model for the effects of the pore pressure are made only during the unloading parts of the stress-strain response.

Conditions of full saturation are assumed to exist throughout the soil profile. Also, it is assumed that, because the earthquake forces are applied so suddenly and for a short time, no flow of pore water takes place, i.e. undrained conditions can be considered.

RESPONSE TO EARTHQUAKE MOTION

The dynamic response of horizontally layered soil deposits was studied using the lumped mass method, in which the deposit is represented as a multi-degree of freedom shear beam. The response at any level of the deposit, due to an earthquake excitation $\ddot{g}(t)$ at the base of the deposit, is obtained by solving the differential equation of motion of the system

$$[M]\{\ddot{x}\} + [C]\{\dot{x}\} + [K]\{x\} = -[M]\{\ddot{g}(t)\} \quad (8)$$

where $[M]$ is the diagonal mass matrix, $[C]$ the viscous damping matrix, $[K]$ the non-linear stiffness matrix and $\{\ddot{x}\}$, $\{\dot{x}\}$, and $\{x\}$ the acceleration, velocity and displacement vectors respectively. In the present analysis only hysteretic damping, inherent in the stress-strain model, has been considered.

Equation 8 is solved numerically using an operator assuming parabolic variation of the acceleration between two successive time steps (Ref.11).

An excerpt from the Temblor N65W strong motion record obtained during the Parkfield earthquake has been used as input earthquake motion at the base of the examined soil profile.

Four case studies were carried out in order to study the effects of a number of parameters on the response characteristics of a soil deposit.

In Case Study No. 1 the response of the deposit was evaluated in terms of total and effective stresses. The results are shown in Fig. 2. It can be seen that the analysis in terms of total stresses shows an amplification of the bedrock motion, while that in terms of effective stresses a depression. It can also be seen that for about the first 1.2 sec. of shaking both analyses yield accelerations of the same order of magnitude. However, in the analysis in terms of effective stresses excess pore water pressures were allowed to develop and by the time of 1.2 sec. the excess pore pressure had reached considerably high values, which led to degradation of the soil stiffness and development of zones of plastic failure. Consequently, the failure zones started to act as a cut-off to the input motion and large strains were induced.

Case study No. 2 was used to study the effects of the bedrock motion intensity on the response characteristics of the deposit. The Temblor N65W acceleration record was used as bedrock motion twice, the second time scaled to maximum acceleration equal to half of the original record. The results are shown in Fig. 3. It can be seen that the maximum surface acceleration due to the weak motion is larger than that due to the strong motion. This can be mainly attributed to the degrading effect, on the soil stiffness, of the development of high excess pore water pressures during shaking. In fact, in a lower level of the deposit, during the initial stages of shaking the strong bedrock motion induces much larger accelerations and consequently larger shear stresses than the weak motion. This resulted in the generation of higher excess pore pressures which in effect degraded the stiffness of the soil and the material was not able to transmit any more large accelerations. At the same time the excess pore pressures in the deposit under the weak motion were low and the material was still strong enough to transmit larger accelerations than the deposit under the strong motion. It has to be noted that the findings of this case study can be applied only to a soil deposit consisting of material with a given potential to develop excess pore water pressures during earthquake shaking, and cannot be generalized.

In Case Study No. 3 the response of two soil deposits, with the same geometric characteristics but different soil properties, were compared. The results are shown in Fig. 4. It can be seen that the "soft" soil deposit transmits smaller accelerations than the "stiff" deposit, at the expense of larger shear strains. The analysis has also shown that the higher excess pore pressure development potential⁽¹⁾ is more critical, from the depression of the input motion point of view, than the softer material (material with low shear strength parameters).

(1) The shear stress ratio τ/σ'_{vo} required to cause liquefaction, i.e. $\Delta u/\sigma'_{vo} = 1$, in one cycle is termed herein as excess pore pressure development potential.

Finally, in Case Study No. 4 the effects of the presence of a mass on the surface of a soil deposit on its response have been studied. The results are shown in Fig. 5. It can be seen that the imposed depression on the input motion, for these site conditions, is much lower than that without surface surcharge. This can be attributed to the stiffening of the soil in the former case, since the soil strength parameters, being dependent on the effective stress level, have been considerably increased due to the presence of the supported mass. It can also be seen that all the high frequencies that exist in the response of the deposit without surcharge have been filtered out. This is because the high frequencies of the deposit with surcharge are much lower than those of the deposit without surcharge.

CONCLUSIONS

An effective stress method for the dynamic response analysis of horizontally layered soils has been developed and used to study the effects of a number of parameters on the response characteristics of a soil deposit. The method is based on the coupling of the dynamic soil response, assumed to be nonlinear, and the pore pressure response.

The analyses reveal substantial differences between the response computed in terms of effective stresses and that in terms of total stresses, the latter overestimating the liquefaction potential of the deposit as well as the induced accelerations and underestimating the induced displacements. There is also a considerable effect of the bedrock motion intensity on the response characteristics of the deposit, and under certain conditions a weak motion can induce larger accelerations than a stronger motion. The results also show that large ground accelerations can be transmitted to a structure only through strong soil deposits. Weak foundation materials act as a cut-off to the transmission of large accelerations on the expense of large displacements. Finally, the presence of a surface surcharge results in the transmission of larger accelerations than the normal case.

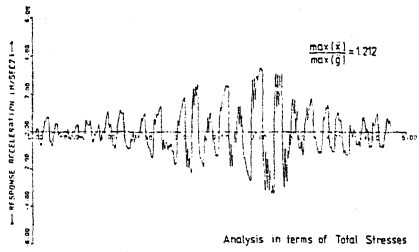
ACKNOWLEDGEMENTS

The support to the second author by the Alexander S. Onassis Foundation is gratefully acknowledged.

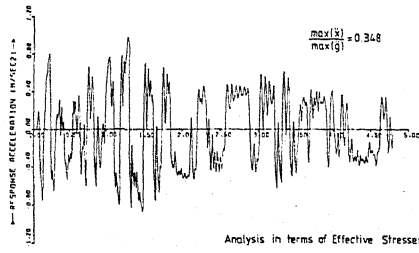
REFERENCES

1. Finn, W.D.L., Byrne, P.M., and Martin, G.R. (1976) " Seismic Response and Liquefaction of Sands", Jrnl. Geot. Engng. Div., ASCE, Vol. 102, No. GT8, Proc. Paper 12323, August, pp. 841-856
2. Finn, W.D.L., Lee, K.W., and Martin, G.R. (1976) "An Effective Stress Model for Liquefaction", Proceedings, ASCE Specialty Session on "Liquefaction Problems in Geotechnical Engineering", Philadelphia, Pa. September 27 - October 1, pp. 169-198.
3. Chaboussi, J., and Dikmen, U. (1977) "LASS-II, Computer Program for Analysis of Seismic Response and Liquefaction of Horizontally Layered Sands", Report No. UIIU-ENG-77-2010, Univeristy of Illinois at Urbana-Champaign, Urbana, Ill.
4. Hardin, B.O., and Drnevich, V.P. (1972) "Shear Modulus and Damping in Soils : Design Equations and Curves", Jrnl. Soil Mech. and Fndns. Div.

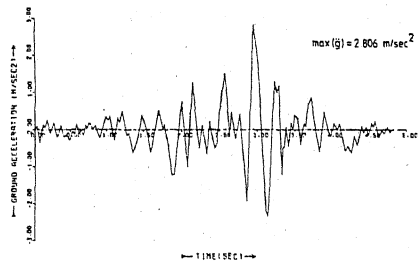
- ASCE, Vol. 98, No. SM7, Proc. Paper 9006, July, pp. 667-692
5. Ishihara, K., and Towhata, I. (1980) "Effective Stress Method in One-Dimensional Soil Response Analysis", Proceedings, 7th Inter. Conf. on Earthquake Engineering, Istanbul, September, Vol. 3, pp. 73-80.
 6. Liou, C.P., Streeter, V.L., and Richart, F.E., Jr. (1976) "A Numerical Model for Liquefaction", Proceedings, ASCE Specialty Session on "Liquefaction Problems in Geotechnical Engineering", Philadelphia, Pa., September 27 - October 1. pp. 313-341.
 7. Martin, P.P. (1975) "Non-Linear Methods for Dynamic Analysis of Ground Response", Ph.D. Dissertation, University of California, Berkeley, Ca.
 8. Martin, P.P., and Seed, H.B. (1979) "Simplified procedure for Effective Stress Analysis of Ground Response", Jrnl. Geot. Engng. Div., ASCE, Vol. 105, No. GT6, Proc. Paper 14659, June, pp. 739-758.
 9. Sarma, S.K., and Jennings, D.N. (1980) "A Dynamic Pore Pressure Parameter A_n ", Proceedings, Inter. Symp. on "Soils under Cyclic and Transient Loading", Swansea, January, Vol. 1, No. 2, pp. 295-298.
 10. Sarma, S.K., and Tsatsanifos, C.P. (1982) "Effective Stress Analysis of a Soil Layer Subjected to Earthquake Loading", Proceedings, 7th European Conf. on Earthquake Engineering, Athens, September 20-25, Vol. 2, No. 4 pp. 523-530.
 11. Tsatsanifos, C.P. (1982) "Effective Stress Method for Dynamic Response Analysis of Horizontally Layered Soils", Ph. D. Thesis, Imperial College, University of London, London.
 12. Tsatsanifos, C.P., and Sarma, S.K. (1982) "Pore Pressure Rise During Cyclic Loading of Sands", Jrnl. Geot. Engng. Div., ASCE, Vol. 108, No. GT2, Proc. Paper 16837, February, pp. 315-319.



Analysis in terms of Total Stresses

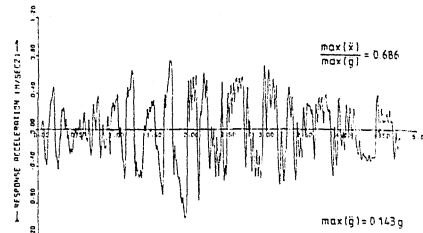


Analysis in terms of Effective Stresses

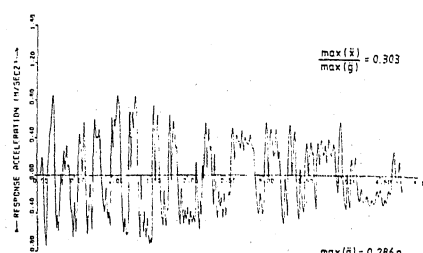


TIME (SEC)

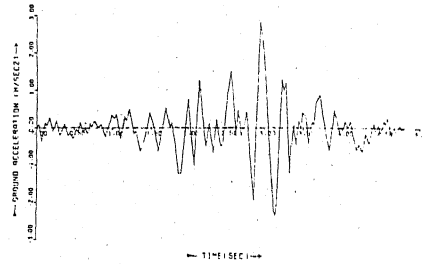
Fig. 2 Surface Acceleration Time Histories
Case Study No. 1



max(g) = 0.143g

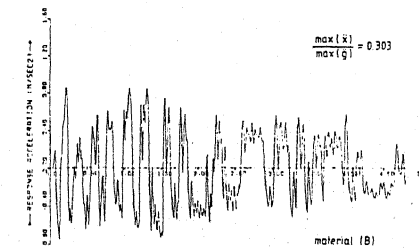


max(g) = 0.286g

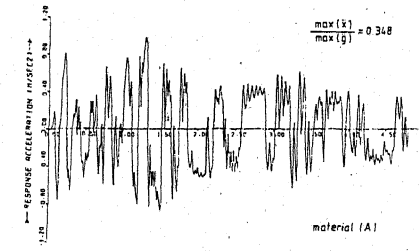


TIME (SEC)

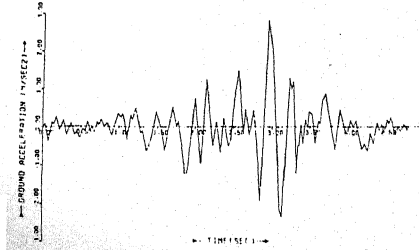
Fig. 3 Surface Acceleration Time Histories
Case Study No. 2



material (B)

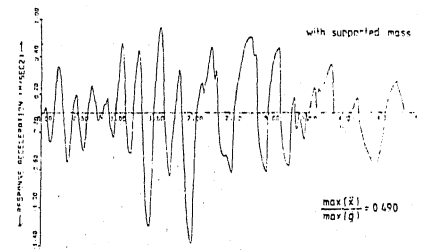


material (A)



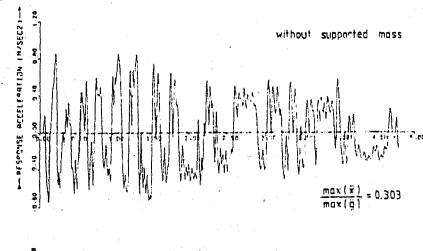
TIME (SEC)

Fig. 4 Surface Acceleration Time Histories
Case Study No. 3



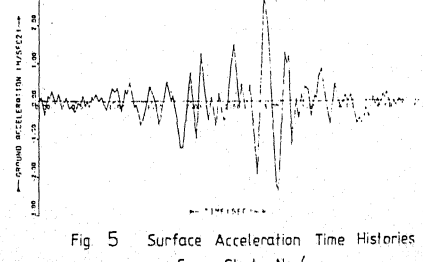
with supported mass

max(x) = 0.690
max(g) = 0.690



without supported mass

max(x) = 0.303
max(g) = 0.303



TIME (SEC)

Fig. 5 Surface Acceleration Time Histories
Case Study No. 4